# Simulating the Midwestern U.S. Drought of 1988 with a GCM

Y. C. SUD, D. M. MOCKO,* K.-M. LAU, AND R. ATLAS

*Laboratory for Atmospheres, NASA Goddard Space Flight Center, Greenbelt, Maryland*

(Manuscript received 24 October 2002, in final form 14 April 2003)

ABSTRACT

Past studies have suggested that the drought of the summer of 1988 over the midwestern United States may have been caused by sea surface temperature (SST) anomalies, an evolving stationary circulation, a soil-moisture feedback on circulation and rainfall, or even by remote forcings. The relative importance of various contributing factors is investigated in this paper through the use of Goddard Earth Observing System (GEOS) GCM simulations. Seven different experiments, each containing an ensemble of four simulations, were conducted with the GCM. For each experiment, the GCM was integrated through the summers of 1987 and 1988 starting from an analyzed atmosphere in early January of each year. In the baseline case, only the SST anomalies and climatological vegetation parameters were prescribed, while everything else (such as soil moisture, snow cover, and clouds) was interactive. The precipitation differences (1988 minus 1987) show that the GCM was successful in simulating reduced precipitation in 1988, but the accompanying low-level circulation anomalies in the Midwest were not well simulated. To isolate the influence of the model's climate drift, analyzed winds and analyzed soil moisture were prescribed globally as continuous updates (in isolation or jointly). The results show that remotely advected wind biases (emanating from potential errors in the model's dynamics and physics) are the primary cause of circulation biases over North America. Inclusion of soil moisture helps to improve the simulation as well as to reaffirm the strong feedback between soil moisture and precipitation. In a case with both updated winds and soil moisture, the model produces more realistic evapotranspiration and precipitation differences. An additional case also used soil moisture and winds updates, but only outside North America. Its simulation is very similar to that of the case with globally updated winds and soil moisture, which suggests that North American simulation errors originate largely outside the region. Two additional cases examining the influence of vegetation were built on this case using correct and opposite-year vegetation. The model did not produce a discernible improvement in response to vegetation for the drought year. One may conclude that the soil moisture governs the outcome of the land–atmosphere feedback interaction far more than the vegetation parameters. A primary inference of this study is that even though SSTs have some influence on the drought, model biases strongly influence the prediction errors. It must be emphasized that the results from this study are dependent upon the GEOS model's identified errors and biases, and that the conclusions do not necessarily apply to results from other models.

## 1. Introduction

The drought of the summer of 1988 over the midwestern United States was a major North American drought. This drought persisted over the agricultural region of the Great Plains during the spring and early summer, and had a devastating effect on crop yields in the Midwest as well as the U.S. economy as a whole (Trenberth and Branstator 1992). Its catastrophic features included: (i) 50%–85% below normal precipitation in midwestern North America, the northern plains, and the Rockies; (ii) record-high surface temperatures; widespread forest fires that burned nearly 4.1 million acres of forests by mid-autumn; (iii) record-low Mississippi River discharge (40% of normal in mid-June 1988); and (iv) a total estimated economic loss of roughly 40 billion dollars. On the basis of this data, it turned out to be the worst drought in the last 40 yr. The drought was accompanied by surface flux anomalies that were huge as compared to changes in surface fluxes of global warming (for example), and yet it is this drought that the general circulation models (GCMs) of our times often fail to simulate.

One can safely infer that SST, soil moisture, and persistence of a stationary circulation are among the key factors in the generation of the midwestern drought of 1988. Of the two earliest studies of this drought, Trenberth et al. (1988), using a linear model and SST data, advocated the SST anomalies to be the primary cause, while Namias (1991) found that deficient precipitation in antecedent seasons and extratropical SSTs were both relevant factors. Canonical ensemble SST correlations of Shen et al. (2002) show how extratropical SSTs in

* Additional affiliation: SAIC/General Sciences Operation, Beltsville, Maryland.

*Corresponding author address:* Dr. Y. C. Sud, Laboratory for Atmospheres, NASA Goddard Space Flight Center, Greenbelt, MD 20771.
E-mail: sud@climate.gsfc.nasa.gov

the North Atlantic have an association with North American rainfall and are responsible for enhanced potential predictability. A 40-yr dataset (1947–86) from Center for Ocean-Atmospheric Prediction Studies (COAPS) analysis was examined (Sittel 1994) that identified the Great Plains regions to be susceptible to warming/droughts in association with cold La Niña episodes. Castro et al. (2001) examined the National Centers for Environmental Prediction–National Center for Atmospheric Research (NCEP–NCAR) reanalysis (1948–98) and showed that La Niña conditions tend to shorten the spring season rainfall in the Great Plains and lead to drier early-summer conditions, a mechanism also suggested as a contributing factor by Namias (1991) and Pal and Eltahir (2001). Atlas et al. (1993) used the Goddard Laboratory for Atmospheres (GLA) GCM to show that prescribing observed tropical SST anomalies and estimated Great Plains soil moisture anomalies greatly improved the 1988 U.S. drought simulation. Since 1988 was a La Niña year, the summer was preceded by significant snowfall anomalies over the northern Rockies. Such evaluations of climatic variables of the Northern Hemisphere as a whole discern the sequence of phases during the ENSO cycles.

Additional studies identified other plausible explanations; Mo et al. (1991) suggested that the initial state of the atmosphere attained a rather stable regime after the third week of May 1988 and continued to support the drought circulation through June regardless of the tropical SST anomalies. These results imply a possible role of soil moisture feedback in creating the drought. Indeed, the study by Pal and Eltahir (2001) delineated the importance of the soil moisture–precipitation feedback for the persistence of the midwestern U.S. drought into the summer. Dirmeyer (1999) and Fennessy and Shukla (1999) found that the impact of soil moisture on precipitation depends on several factors (such as extent–magnitude–persistence of the soil moisture change and the regional dynamical circulation) and that realistic soil moisture enhances seasonal predictions. Land feedbacks such as surface albedo (Sud and Molod 1988) and vegetation variations (Sud et al. 1993, 1995) have been shown to produce a positive feedback on a drought circulation and rainfall; however, they do not help much in explaining or understanding transient droughts.

A study by Fox-Rabinovitz et al. (2001) identified the importance of higher model resolution over the continental United States for a better simulation of the circulation and rainfall in a stretched-grid GCM. Fennessy and Shukla (2000) used nesting instead of a stretched grid; they also found that higher resolution invoked with a nested Eta model improved the rainfall prediction for the drought (1988) and flood (1993) years of North America. This shows that high resolution helps to produce a better prediction. Some successes with regional models run with observed lateral data have been documented (e.g., Giorgi et al. 1996; Hong and Pan 2000; Jenkins and Barron 2000), but the question remains: how does one obtain reliable lateral forcing data to predict such a drought?

Except for the Namias (1991) analysis, all the other studies of the summer 1988 drought are modeling studies; naturally, their inferences would be model-dependent. With every major model improvement of the Goddard Earth Observing System (GEOS) GCM (and its earlier versions), we attempted to simulate the North American drought of summer 1988, but thus far have had only limited success (e.g., Mocko et al. 1999). Naturally, these failures have provided a daunting challenge to determine whether it is the model, the boundary forcings such as soil moisture, or the hard to simulate pathway of the climate system that causes these failures. Are the model's biases, or the soil moisture, or remote forcing errors, or the poor representation of convection the key contributing factors to the model's inability to simulate this drought? After nearly a 15-yr time lapse, we are still expecting to find a good explanation for the lack of predictability of this drought in a free-running GCM. It would be interesting to determine what is missing in the model and how various aspects of model-simulation deficiencies might interact with each other to cause the model's failure. In this study, we shall explore the key observational features of the drought of 1988 and the primary reasons for lack of (or limited) success in simulating it.

Some applications of this investigation could be used in preparation for ENSO-related drought and forest fires as well as provide diagnostic guidance for GCMs to better simulate key features of the observed climatic episodes. In other words, if El Niño/La Niña anomaly is all one can hope to simulate in advance, then the most one can expect to simulate are the circulation features related to it. Also, one can benefit from a similar analysis of other forcing datasets such as soil moisture, snow/ice cover, and vegetation.

The Climate Analysis Center at NCEP [formerly, National Meteorological Center (NMC)] has highlighted some key dynamic features of the drought of 1988 to show how the drought persisted. The jet stream in the Midwest was located far north of its normal position in association with an anomalous ridge of high pressure in the northern plains. This led to northward transport of moist air masses along the west coast of North America making the region rainy and damp. In addition, the high pressure system over the Great Plains caused the low-level jet (normally bringing the Gulf moisture into the Great Plains region) to weaken, thereby shutting off the moisture supply to the region. In fact, this low-level jet is so important that in other recent droughts over midwestern North America, for example, summer of 2000, weakening of the low-level jet and the resulting reduction in moisture transport was a key factor in the production/maintenance of the droughts. The accompanying sea level pressure picture for June–July–August (JJA) of 1988 minus 1987 (Fig. 1) shows high pressure

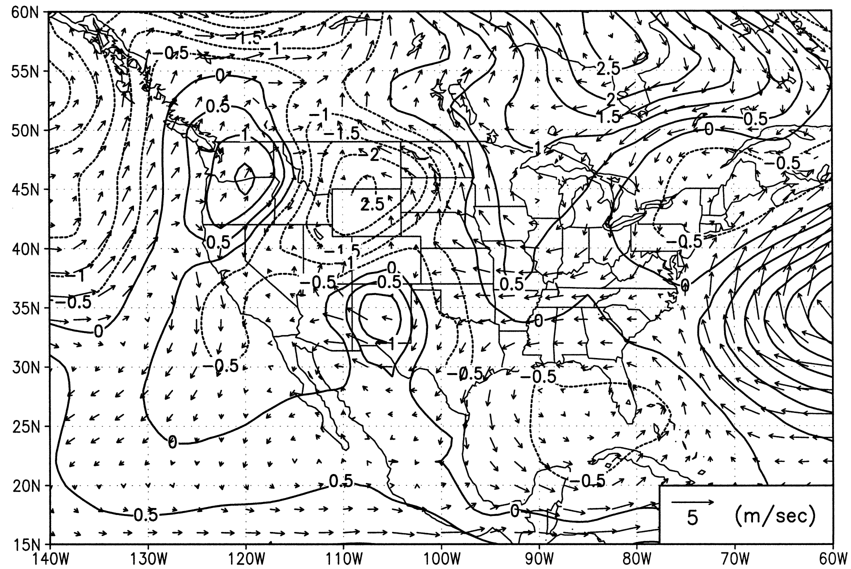


FIG. 1. The 1988 − 1987 JJA sea level pressure (hPa) and surface to 800-hPa averaged wind vectors (m s$^{-1}$) from the GEOS-1 reanalysis.

over Canada was primarily responsible for bringing in dry air from the north. Together with a cyclone over the northern Rockies and an anticyclone to its south, one notes a weakening of the low-level jet. In this way, the low-level jet carrying moisture-laden low-level air from the Gulf of Mexico was replaced with dry air from northern Canada. Such a dynamic scenario would naturally lead to a drought. The drought had its greatest impact in the northern Great Plains. It intensified in this region and spread across much of the eastern half of the United States with total precipitation for April–June of 1988 being lower than the Dust Bowl period. In addition to dry conditions, heat waves during the summer of 1988 broke long-standing temperature records in many midwestern and northeastern metropolitan areas. The drought of 1988 persisted through the early summer and then started to fade away in the late summer when the low-level jet strengthened again and copious rains returned to the region. Further analysis of the physical processes of the drought can be found in Trenberth and Guillemot (1996).

The normalized difference vegetation index (NDVI) analysis from the spring and summer of 1988 in the International Satellite Land Surface Climatology Project (ISLSCP) Initiative I data (Meeson et al. 1995) identifies the drought region experiencing a reduction in rainfall. The extent of the drought region has a remarkable resemblance to the pattern identified in the aforementioned COAPS analysis as regions experiencing a reduction in rainfall in response to La Niña SST conditions. This would suggest that the SST anomaly of 1988 had a causal (at least significant) role on the production of the Great Plains drought. For simulating the influence of drought–SST interactions, observed SST anomalies could be provided to the model. If SSTs were important, a model of some reasonable credibility would be expected to simulate the drought.

Another forcing parameter implicated in some studies (Karl et al. 1993) is the reduced winter snow cover in the northern Rocky Mountains leading to low soil moisture and reduced Mississippi River flow, irrigation, and regional evapotranspiration. One can hope to capture some of these effects through soil moisture and snow cover initializations produced under the Global Soil Wetness Project (GSWP; Dirmeyer et al. 1999), while the influence of the vegetation–drought feedback can be assessed by comparing simulations made with observed vegetation data versus climatological vegetation data. In this way, the model can better capture the influence of realistic soil moisture and vegetation.

In this paper, we also draw upon wind initialization using the analysis of observations produced with the GEOS-1 version of the Data Assimilation Office (at Goddard Space Flight Center) Data Assimilation System (DAO-DAS; Schubert et al. 1993). Presumably, the recent model improvements in the land hydrology/snow and precipitation processes can be expected to better simulate the 1988 drought. These tools and datasets provided the ultimate motivation for this attempt to simulate the midwestern North American drought of summer 1988.

The Goddard Earth Observing System GCM at the Goddard Laboratory for Atmospheres (Conaty et al. 2001) is a general-purpose model used for climate studies and data assimilation. It can be integrated with coupled land and prescribed sea surface temperatures. A climate version of the GCM is often used to simulate climate change and its biogeophysical consequences consistently, even when the GCM does not capture some of the features of a specific climatic episode. There can be several causes for a model's failure to accurately simulate an observed climatic episode. Among them are coarse resolution, simplifications in the representation of atmospheric physics (the primary cause of intrinsic model deficiencies particularly due to parameterizations), and the potential natural variability of the simulated as well as observed climate system. The natural variability of climate is a major source of unpredictability. Consequently, one must view observations as a single realization amongst a host of possible climate pathways in nature that a particular initial state might have produced. Regardless, as research tools, GCM simulations can help us understand and discern the roles of coupled land–atmosphere–ocean interactions in maintaining and modulating the evolving climate of the earth, which includes major hydrological events such as droughts and floods.

Next, section 2 describes the model used in this study. The design of the experiment is detailed in section 3. Simulation results and analysis are presented in section 4, and discussion and conclusions are found in section 5.

## 2. Model description

The version of the GEOS GCM employed in this study had a 2° latitude × 2.5° longitude × 20-sigma-layer resolution. The three key components of the model are hydrodynamics, atmospheric physics including clouds and radiation, and earth–atmosphere interactions including air–sea interaction, biosphere, and hydrology. The hydrodynamics are on a C grid (Takacs et al. 1994) with sigma layers in the vertical. This hydrodynamics has appropriate filters to eliminate 2-$\Delta x$ modes of the dynamical atmosphere and topography (that would generate them) and the pole problems. The recent developmental history of the model includes some major refinements and upgrades to its physical processes such as radiation and new biospheric and boundary layer parameterizations, as well as substantially higher horizontal and vertical resolution than used here. Other key features of the GEOS GCM are: (i) the ability to perform coordinate translation and rotation with a proviso for relocating the mathematical poles to any arbitrary location (not used in this investigation); and (ii) inclusion of a gravity wave drag parameterization due to Zhou et al. (1996). Its land surface model is the so-called HY-SSiB [Simplified Simple Biosphere model (SSiB) from Xue et al. (1991), upgraded with hydrology and snow physics, Sud and Mocko (1999) and Mocko and Sud (2001)]. The convective parameterization of the GCM is the Microphysics of Clouds with Relaxed Arakawa–Schubert Scheme (McRAS; Sud and Walker 1999a,b). These packages were summarized in a recent paper by Sud et al. (2002). The cloud-ice fraction is diagnosed as a linear function of temperature—it is zero at 253.15 K and grows to unity at 233.15 K. When both ice and water clouds coexist, the optical thickness of the mixture is the sum of the mass fraction-weighted optical thickness of both cloud species. The boundary layer scheme for turbulent transport is by Helfand and Lebraga (1988). The radiation package of McRAS is due to Chou and Suarez (1994) with a provision for handling prognostic clouds and in-cloud water and ice fractions (Chou et al. 1998, 1999). The radiation is not too different from that of the original version of the GEOS GCM, except for a revised calculation for the optical thickness of clouds for short- and longwave radiation. For a more detailed description of different modules and parameterizations, the reader may refer to the original papers given as references.

In addition to running the model with interactive physics and full dynamical responses of all the prognostic variables, the wind and/or soil moisture analysis data was inserted into the model for several cases. The wind data was taken from the DAO analysis produced at the same resolution and virtually using the same model. Additionally, analyzed soil moisture data, which was produced in a GSWP-like manner using the offline HY-SSiB model at the same 2.0° × 2.5°. The soil moisture data is available at three levels: surface (diurnal) layer, root zone (seasonal), and deep (recharge) level. The insertion of analyzed data is performed in a straightforward way using a direct insertion approach, that is, simply replacing the simulated fields with the analyzed one at the appropriate time interval at which the analyzed data were available. The final two cases in this study used ISLSCP vegetation parameter data, in place of the GCM's vegetation climatology.

## 3. Design of the experiment

The majority of GCMs employed soon after the drought were unsuccessful in simulating the 1988 drought over North America (e.g., Fennessy et al. 1990), and very little new evidence of better success has emerged ever since. It is, therefore, important to understand its reason(s). Recently, Lau et al. (2002) showed that potential predictability of summer season rainfall anomalies over the continental United States is derived from SST anomalies of the North Pacific even more than that of the tropical Pacific (La Niña events). This suggests that coupled air–sea interactions in the extratropics may be vital to enhance summer season predictions over the United States. Since the emphasis often has been on tropical sea surface temperature anomalies, simulations often deploy tropical anomalies as Niño-1, -2, and -3. This is circumvented in our study because we prescribe the observed SST everywhere. In all our simulation experiments, the best estimates of the observed SSTs were used. Moreover, we specifically designed our simulation experiments to differentially discern the influence of local, internal dynamical, and large-scale external forcings on the model-simulated circulation and rainfall. We have conducted seven sets of simulations as described in the following:

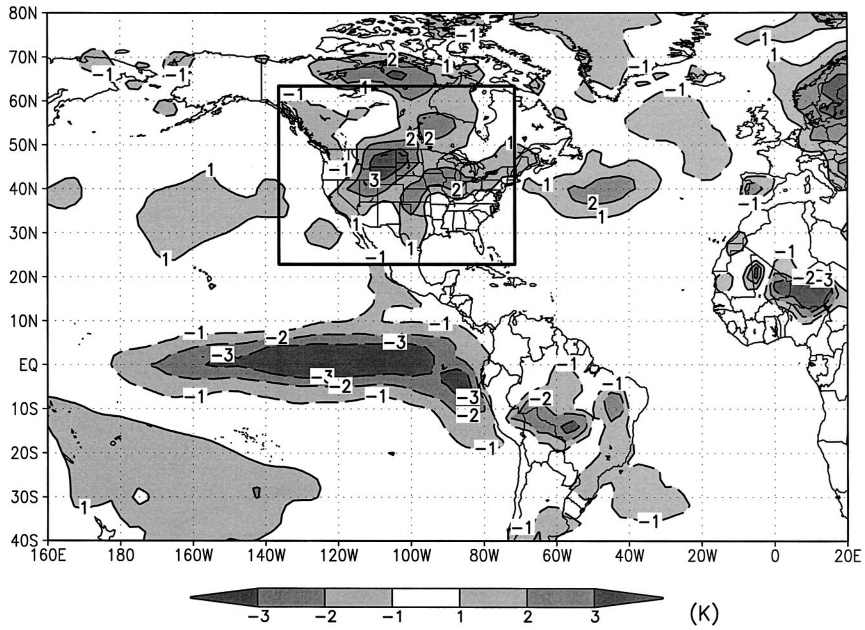


FIG. 2. The 1988 − 1987 JJA surface air temperature (K) from the GEOS-1 reanalysis. The region inside the rectangle over North America from 23°–61°N and 129°–66°W is allowed to freely vary as described in the LBOX experiment. Negative differences are surrounded by a dash.

Case 1 (C1–CTRL): A free-running model integration with prescribed SSTs, while everything else was fully interactive and prognostic;

Case 2 (C2–WIND): Model integrations ingesting DAO-analyzed winds (replacing simulated) at 6-h intervals at all grid points;

Case 3 (C3–SOIL): Model integrations ingesting GSWP-analyzed soil moisture (replacing simulated) once a day at all grid points;

Case 4 (C4–BOTH): Model integrations that ingested both analyzed winds and soil moisture as in C2 and C3;

Case 5 (C5–LBOX): Model integrations are the same as in C4, but with analyzed wind and soil moisture fields only getting ingested outside the limited-area region shown in Fig. 2; the figure also shows the La Niña cool anomaly over the tropical Pacific in 1988, as well as the warmer surface temperatures over North America in the GEOS-1 reanalysis;

Case 6 (C6–VEGI): Model integrations in which C5 was modified with additional insertion of observed vegetation parameters [vegetation cover fraction, greenness, leaf area index (LAI), surface albedo] from the ISLSCP data (as opposed to the GCM's climatological vegetation data) within the region of study;

Case 7 (C7–OPPO): Model integrations in which C6 was updated with the insertion of the opposite year's vegetation parameter data (1988 LAI was used for the 1987 simulation and vice versa).

Each case contained an ensemble of four simulations that started from four consecutive days at 0000 UTC 30, 31 December 1986 and 1, 2 January 1987; and 0000 UTC 30, 31 December 1987 and 1, 2 January 1988. Each simulation was analyzed from 1 June–31 August periods of 1987 and 1988, respectively. In highly constrained simulations, such as C2 in which simulated winds were replaced with the analyzed, the intraensemble variability was very small as expected and as evident in the analysis of model output. For each simulation, the initial conditions of the atmosphere were interpolated from ECMWF analysis, whereas soil moisture and snow cover were taken from the GSWP-style offline HY-SSiB analysis (Sud and Mocko 1999). In all cases, the SST (prescribed as monthly data) was interpolated to produce a slowly varying daily SST using a linear interpolation. Therefore, C1 simulations really represent the model's response to SST anomalies (warm episode of 1987 and cold episode of 1988), plus some influence of the initial soil moisture and snow cover prescribed at the beginning of the year. If the model were a perfect simulator of the earth–atmosphere system, one would expect the soil moisture to evolve realistically. However, this has not been achieved successfully in any simulation, and we believe it relates to the unpredictability of weather. Since weather affects both rainfall episodes and soil moisture, we did not expect the C1 simulation to significantly improve upon the model's inability to simulate the correct land surface boundary forcings for the drought of 1988. Indeed, we were surprised to find that the model did pick up some large-scale features of the circulation that reflect the existence of the drought of 1988 as seen in the 1988 minus 1987 JJA differences (discussed in section 4). Case C2 constraints the moisture transport but not the convergence, which is largely determined by the heating fields generated by the model's physics. Since the soil moisture is an important forcing that is crucially affected by the precipitation and is the first feedback that shows large biases in response to erroneous precipitation, we decided to provide the soil moisture from the HY-SSiB integration in case C3. Thus, case C3 generated a set of simulations for 1987 and 1988 in which everything was the same as in case C1, except that the soil moisture was updated on a daily basis. Since these two insertions had a beneficial effect individually, we replaced both winds and soil moisture with the analysis data in case C4. We expect that if slowly varying boundary forcings have some useful value, this case, with the correct forcings, would produce a better forecast than each of the other three: C1, C2, and C3. Subsequently, we ran case C5 to examine the influence of replacing soil moisture and wind outside the limited-area region. The influence of using ISLSCP vegetation data from the correct and wrong years was assessed in cases C6 and C7, respectively. These simulations helped us to discern: (i) the factors that influenced the drought of the summer of 1988; (ii) the influence of wind and soil moisture biases; (iii) the influence of the wind and soil moisture biases that convey into the region from outside; and (iv) the advantage of using observed as opposed to the climatological biosphere. We shall describe the results in the next section.

## 4. Results

We will describe each of the seven simulations while comparing them with one another and evaluating them vis-à-vis the analyzed data, so-called best estimate of observations. All of the analysis in Figs. 3 through 9 will be shown for time-averaged June–August fields. Since there were four cases in each set of ensemble simulations, all results are presented as ensemble averages unless specifically stated otherwise.

### *a. Case C1: Control simulation*

Based on the $2.0° \times 2.5°$ horizontal resolution of the GEOS GCM employed for the study, we would expect to simulate only the synoptic-scale character of circulation changes that are forced by the observed SST and evolving soil moisture, snow cover, and land hydrology anomalies. Figure 3a shows the 200-hPa streamfunction of 1988 minus 1987 for the JJA period simulated by the GCM (Fig. 3a, top) in case C1 vis-à-vis the same fields from analysis of observations produced by DAO Data Assimilation System (DAS) (Fig. 3a, bottom). Positive (negative) differences in streamfunctions over the northern midlatitudes (Tropics) are evident in both plots. The model simulates a positive streamfunction anomaly over the drought region of North America (Fig. 3a, top) that has some synoptic-scale resemblance with analyzed data for the same period. The similarity of these large-

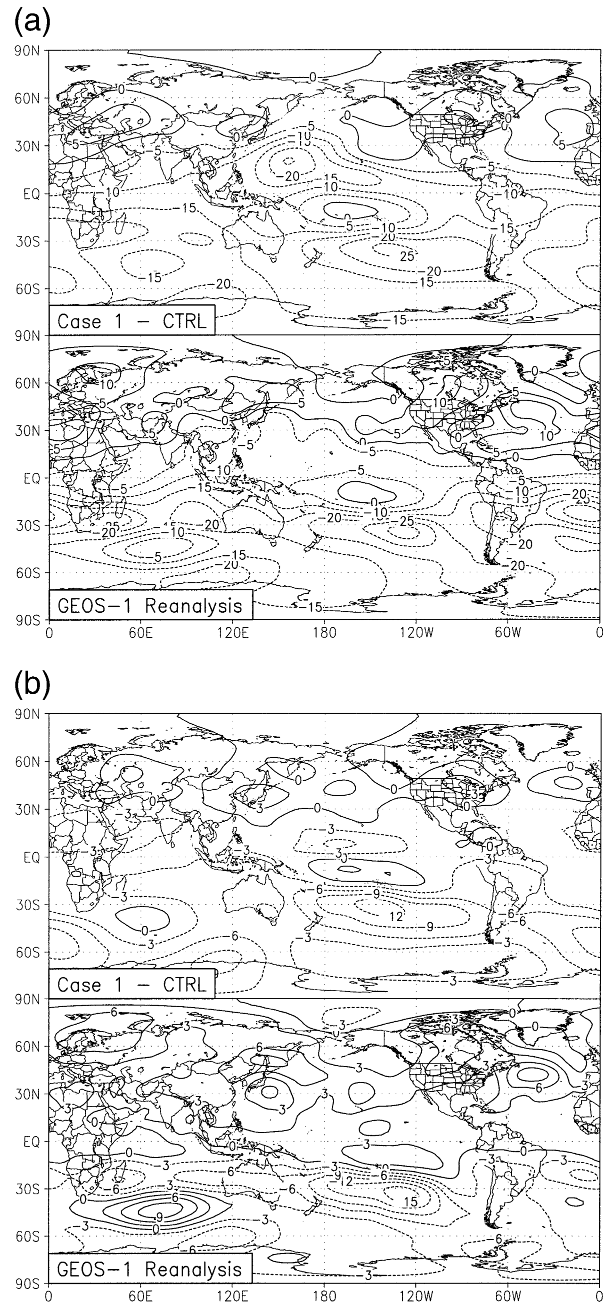


FIG. 3. (a) The 1988 − 1987 JJA 200-hPa streamfunction ($10^{10}$ kg $s^{-1}$) from (top) case C1 CTRL, and (bottom) GEOS-1 reanalysis. (b) Same as in (a) only for 500-hPa streamfunction.

scale patterns indicates that the model has some skill at those scales. A similar examination of streamfunction differences between simulated and analyzed data at the 500-hPa level (Fig. 3b) again shows some resemblance between them. These two figures suggest that the model has some skill in prediction of the very large scales in C1.

Let us now examine the North American circulation and rainfall. There are large differences between case

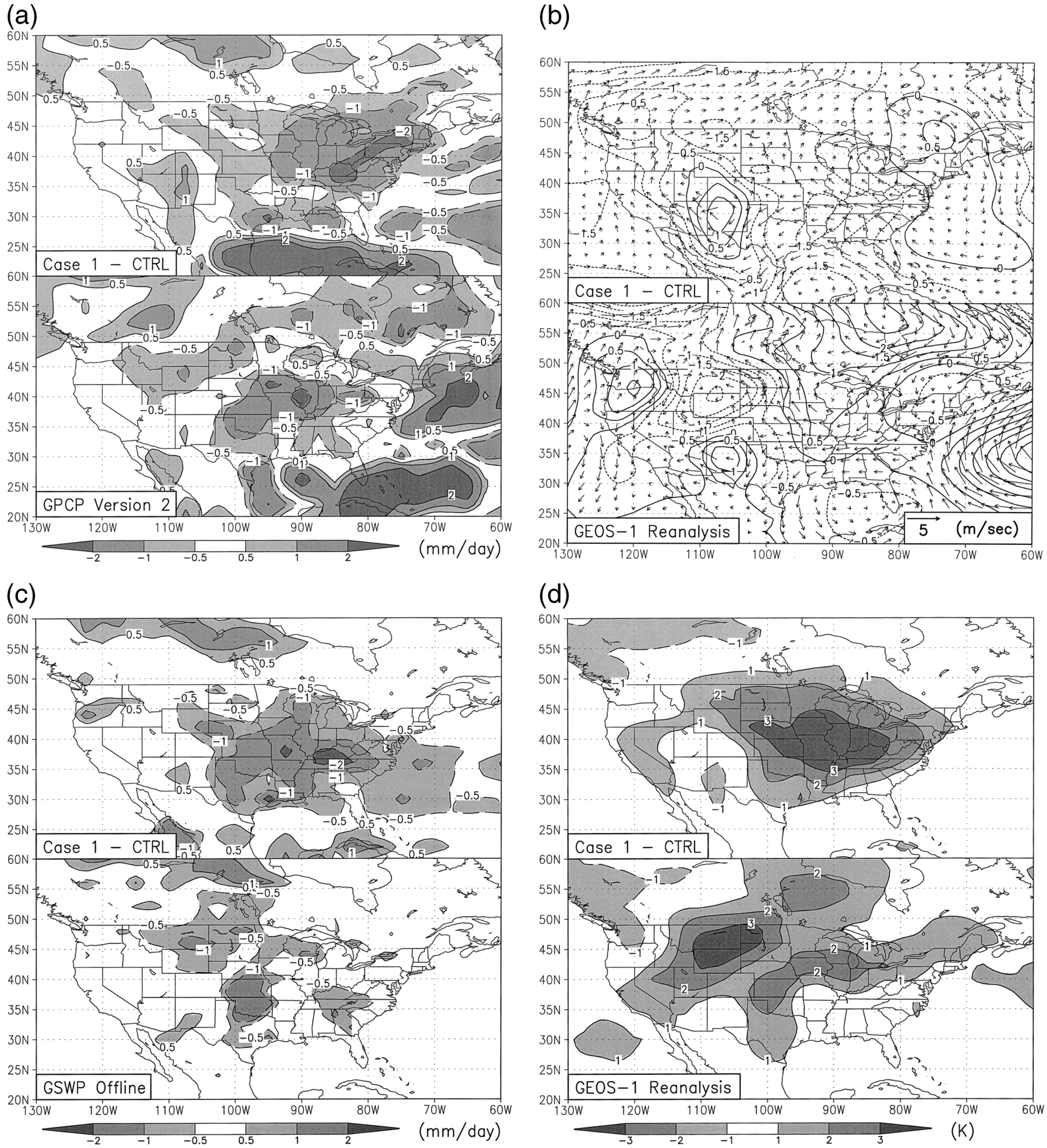


FIG. 4. (a) The 1988 − 1987 JJA precipitation (mm day$^{-1}$) from (top) case C1 CTRL, and (bottom) GPCP version 2. Negative differences are surrounded by a dash. (b) The 1988 − 1987 JJA sea level pressure (in hPa) and surface to 800-hPa averaged wind vectors (in m s$^{-1}$) from (top) case C1 CTRL, and (bottom) GEOS-1 reanalysis. (c) The same as in (a) except for evaporation (mm day$^{-1}$) and (bottom) for GSWP offline. (d) Same as in (b) only for surface air temperature (in K). Negative differences are surrounded by a dash.

C1 and the Global Precipitation Climatology Project (GPCP) rainfall fields (Huffman et al. 1997) as shown in Fig. 4a. The model simulates a drought in JJA of 1988 in the midwestern to eastern United States with 1–2 mm day$^{-1}$ reduction in rainfall while the GPCP analysis has a less widespread reduction. On the other hand, the observations have many smaller-scale details than the smoothed field of the GCM, which is a member average at 2.0 by 2.5 resolution. In comparing the surface to 800-hPa wind fields and sea level pressure (Fig. 4b), one finds that the circulation and sea level pressure (SLP) shown in the form of 1988 minus 1987 differ-

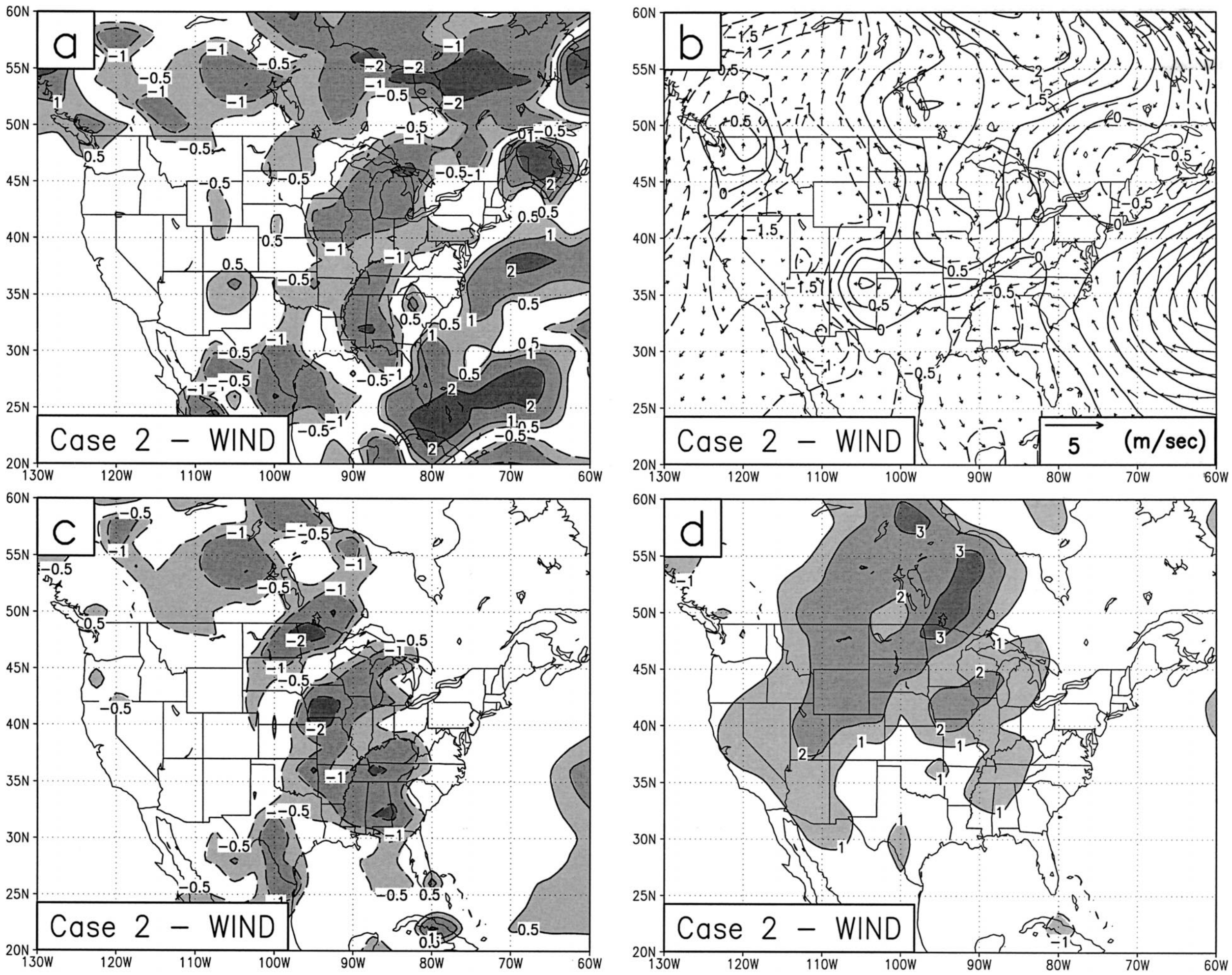


Fig. 5. Same as in Fig. 4 only for case C2 WIND.

ences reveal that the control simulation is unable to simulate the details of the near-surface circulation and divergences. Consequently, all precipitation pattern and circulation anomalies are quite different between the model and the analysis of observations. From this, one infers that whatever drought is simulated in the 1988–87 rainfall fields, the discernible character of the 1988 minus 1987 circulation does not accompany it. The dominant influence is the large-scale control exerted through the observed SSTs, evidenced in the 200- and 500-hPa anomaly patterns. The model does simulate a drought in 1988 that also affects the evapotranspiration (Fig. 4c) and surface temperature (Fig. 4d). Both of these fields indicate that the GCM is drier and warmer than observed; presumably, it is a consequence of a positive feedback between soil moisture and surface temperature. Excessive evapotranspiration is likely to cause decreasing soil moisture and higher temperatures, particularly in the summer. However, it would appear that the model does simulate some sort of a large-scale drought in JJA of 1988 with respect to 1987. Such a forecast could be useful, but its biases and missing details raise many questions about its value for agriculture and water resource management.

Table 1. The 1988 − 1987 monthly and JJA precipitation correlation between GEOS precipitation for all cases and GPCP version 2 for the North American region of 23°–61°N, 129°–66°W.

| | Jun | Jul | Aug | JJA |
|---|---|---|---|---|
| Case 1–CTRL | 0.170 | 0.020 | 0.140 | 0.171 |
| Case 2–WIND | 0.592 | 0.332 | 0.429 | 0.558 |
| Case 3–SOIL | 0.175 | 0.357 | 0.180 | 0.245 |
| Case 4–BOTH | 0.609 | 0.356 | 0.448 | 0.546 |
| Case 5–LBOX | 0.369 | 0.288 | 0.353 | 0.417 |
| Case 6–VEGI | 0.389 | 0.283 | 0.395 | 0.421 |
| Case 7–OPPO | 0.386 | 0.304 | 0.403 | 0.444 |

### *b. Case C2: Wind updated from analysis*

We next examine the influence of local, synoptic-scale and collateral errors on the JJA circulation and rainfall. This is done in the simulation experiments C2 through

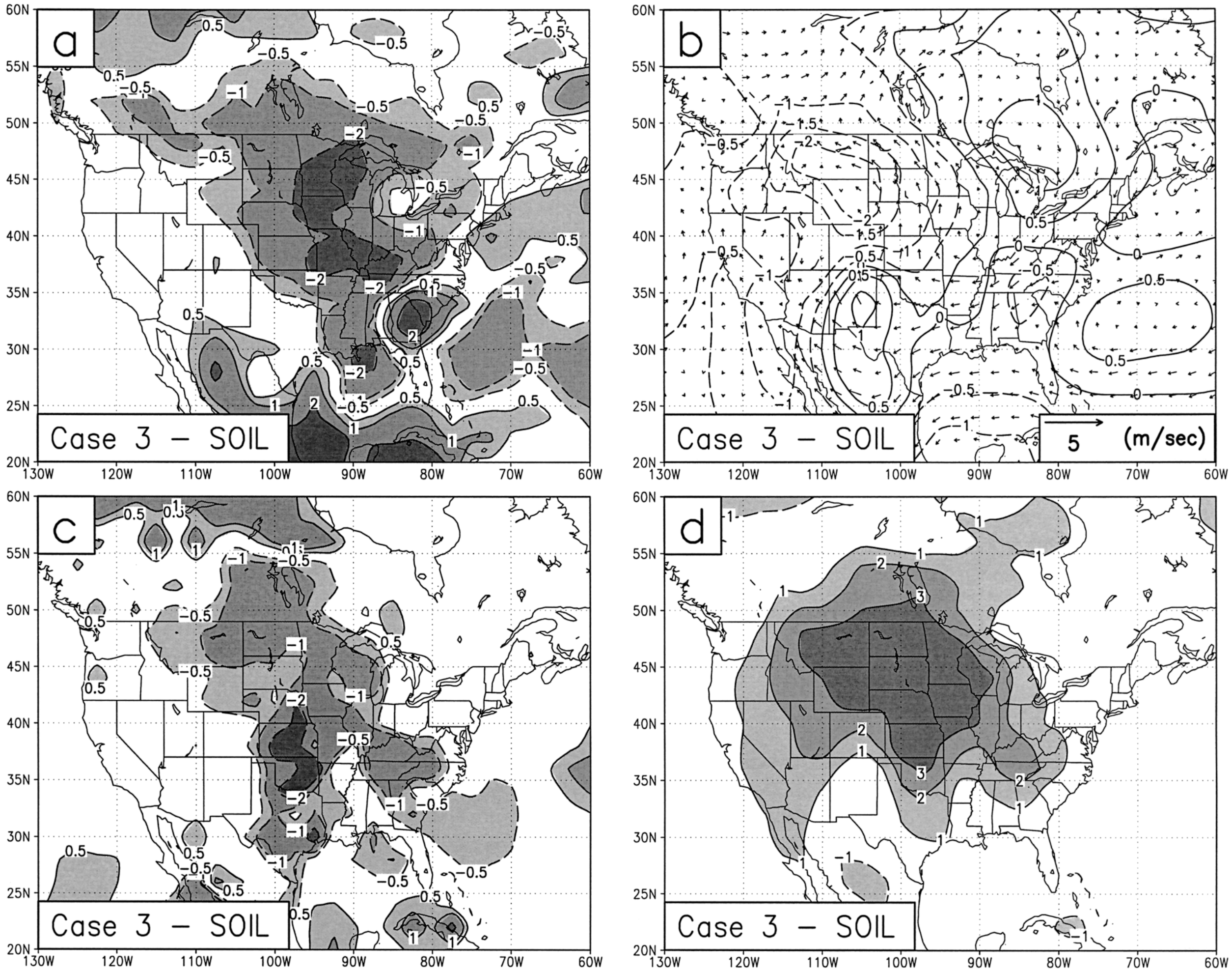


FIG. 6. Same as in Fig. 4 only for case C3 SOIL.

C7. Case C2 represents a simulation in which the simulated winds are replaced by the observed at 6-h intervals. Any horizontal wind field has two components: one is divergent and the other is rotational. The updated winds would directly alter the rotational part, but the divergent part will be determined by the model's diabatic heating fields, particularly the temperature (which is not updated) and its effect on associated divergence (because the temperature change indicated heating, which affects divergence). The rotational parts of the winds do not change much in response to heating, but they help to transport heat and moisture as well as alter the pressure gradients to establish the geostrophic (vorticity–pressure) relationship. With observed winds, the model must capture the observed transports while it can modulate its divergences in response to diabatic heating fields produced by the model's physical interactions. Over a short time period, dynamics generally overwhelms the physics; therefore, by inputting observed winds, the dynamics gets constrained everywhere, whereas thermodynamics has some freedom to influence the temperature and vertical velocity fields according to the model's physical parameterizations.

Naturally, C2-simulated 1988 minus 1987 precipitation fields (Fig. 5a) are improved over the result from C1. In order to quantify this improvement, the spatial correlation between the ensemble-averaged simulated precipitation for all cases and the GPCP precipitation for June–July–August is shown in Table 1. More striking is the improvement in sea level pressure (Fig. 5b) (surface to 800-hPa motion fields as prescribed), which is in much better agreement with observations. There was virtually no difference in any fields including precipitation among the members of the ensembles. The evapotranspiration patterns (Fig. 5c) also had a strong resemblance among the members. Any differences can be either due to soil moisture anomalies, to radiative forcing, or to any remaining SSiB deficiencies in the simulation of the entire biosphere–land-hydrology complex. Comparison of differences over the ocean with offline GSWP data is not meaningful because GSWP does not apply over the oceans. The accompanying surface temperature

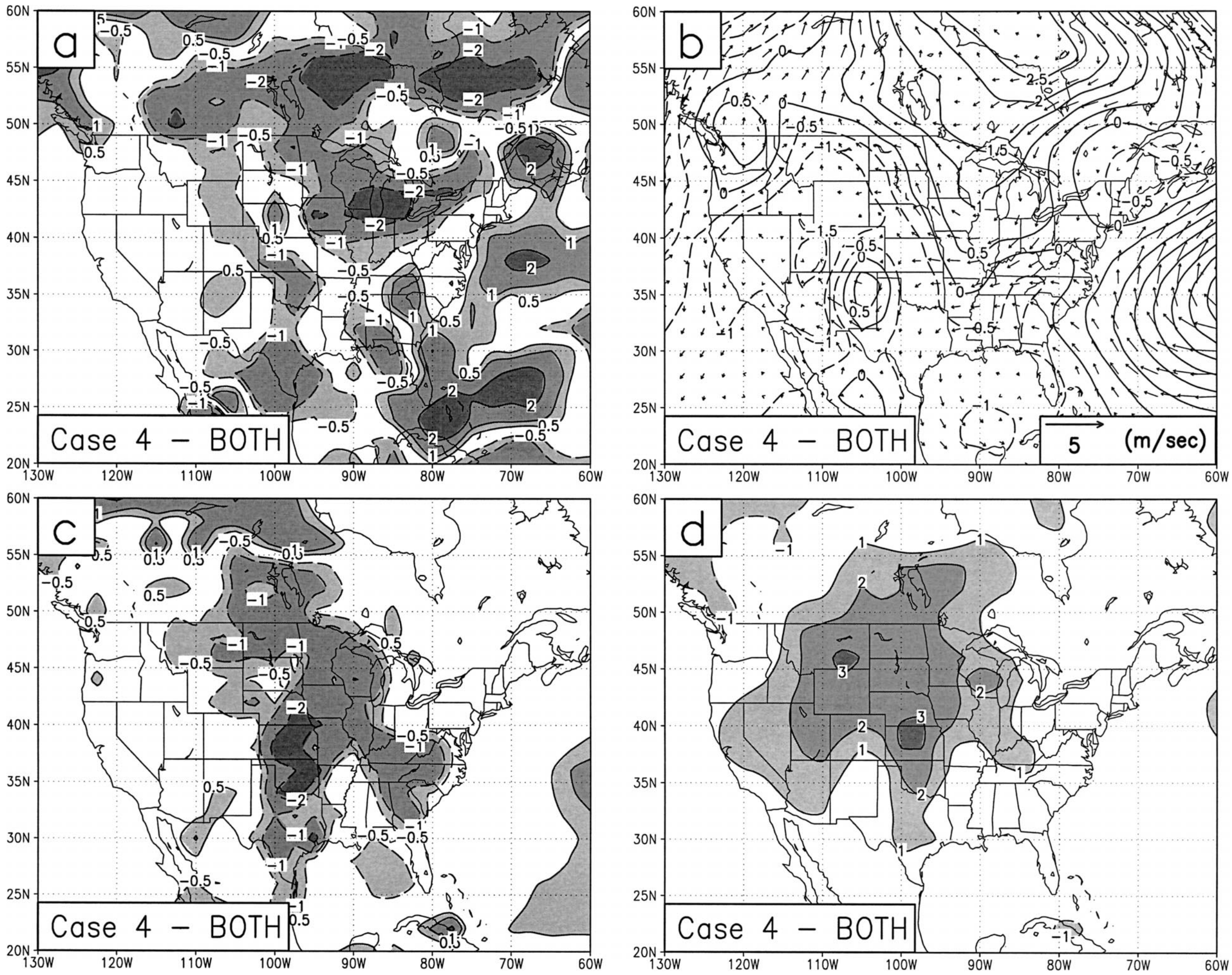


FIG. 7. Same as in Fig. 4 only for case C4 BOTH.

differences (Fig. 5d) are consistent with the evapotranspiration differences, with somewhat better resemblance to GSWP and GEOS-1 reanalysis fields (Figs. 4c and 4d). Comparison of simulated soil moisture to the GSWP soil moisture for this case indicated that the soil moisture was generally drier for C2 than for C1. Overall, we note that wind errors in the chosen region are responsible for most of the synoptic-scale errors. This suggests that one can benefit substantially by having a forecast system in which winds are properly initialized and/or better simulated. This is in agreement with a number of previous studies (e.g., Atlas et al. 2001) in which winds are considered vital for the accuracy of weather forecasts.

### *c. Case C3: Soil moisture updates from GSWP analysis*

In case C3 we used the GSWP-analyzed soil moisture only; it was performed by replacement of simulated soil moisture with the offline analyzed fields (Meeson et al. 1995) at each grid point at 0000 UTC (once a day). An examination of the sea level pressure and surface to 800-hPa winds, evapotranspiration, and surface temperature fields (Figs. 6b–6d) shows that the soil moisture slightly improved the simulation over Case C1. The precipitation anomaly distribution (Fig. 6a) was shifted westward, making it more realistic, albeit too strong compared to observations. This improvement is also noted in Table 1. The model's patterns represent a combination of soil moisture and net radiative forcing and circulation. At least over the drought regions, reduced soil moisture has produced warmer temperatures even though the synoptic-scale surface to 800-hPa circulation remained largely unaffected.

### *d. Case C4: Both wind and soil moisture updates*

In C4, both winds and soil moisture were updated from analysis of observations. Precipitation differences

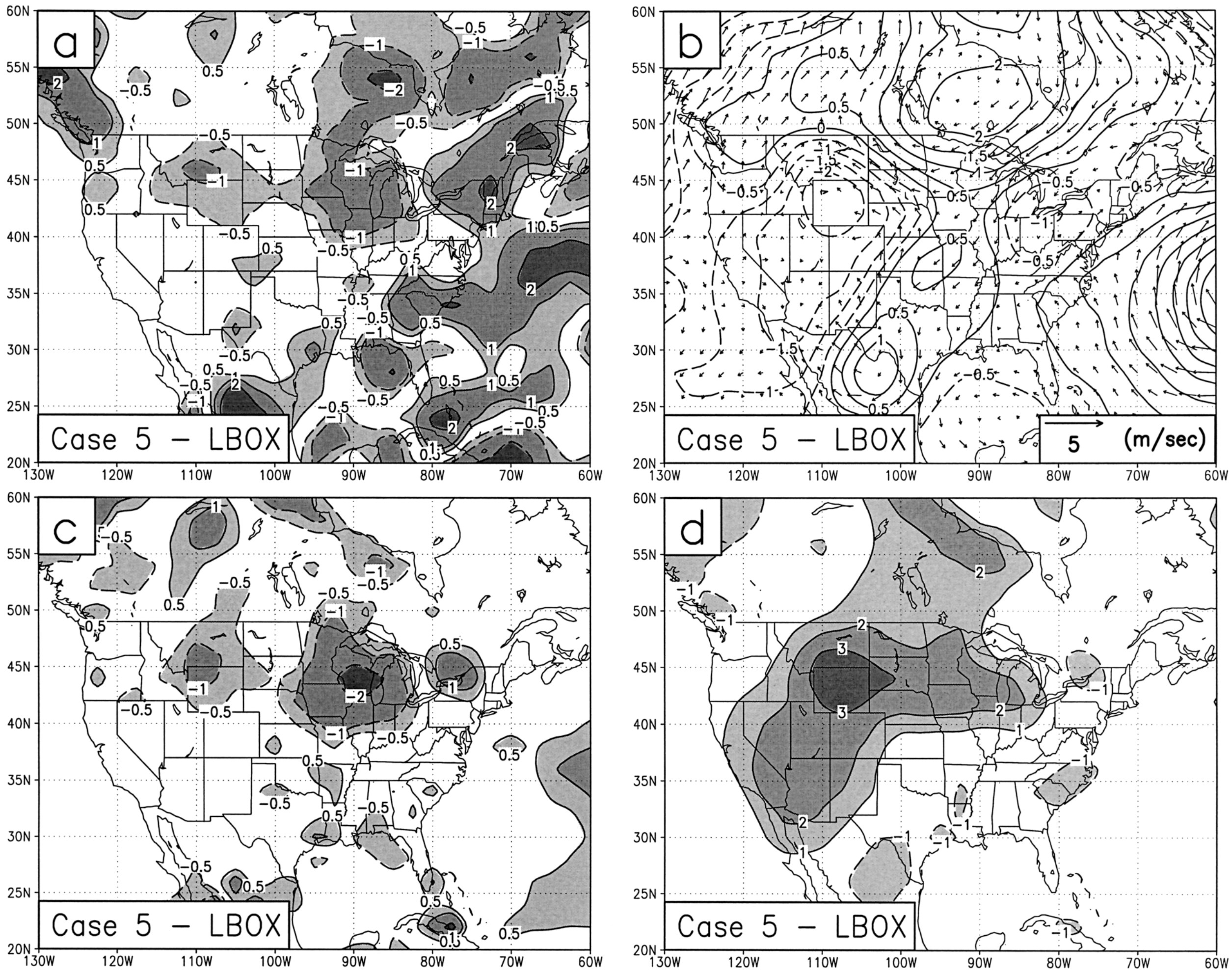


FIG. 8. Same as in Fig. 4 only for case C5 LBOX.

(Fig. 7a) have a much closer resemblance with GPCP rainfall differences (Fig. 4a). As expected, most of the benefits were derived from input of observed winds. Soil moisture benefits were relatively smaller in this comparison. The SLP changes (Fig. 7b) are similar to those of C2 and the influence of analyzed soil moisture in not discernible in the JJA average. However, in the case of evapotranspiration anomalies (Fig. 7c), the combined simulation is similar to the soil moisture anomaly simulation C3 (Fig. 6c). This shows that soil moisture must be more important than the wind for evapotranspiration, which is a major component of surface energy fluxes. In that way, the current result makes good intuitive sense. A clear difference is in the surface temperature anomaly pattern (Fig. 7d). They are similar to the surface temperature patterns of C3 (Fig. 6d), but the intensity of differences is much reduced and the values are in better agreement with the analysis. In this way, the use of observed winds helps transport the air mass and its associated temperature more realistically as compared to the soil moisture update only, case C3.

### *e. Case C5: Winds and soil moisture updates outside LBOX*

Case C5 represents simulations with both soil moisture and wind fields updated, but only outside of the region of 23°–61°N and 66°–129°W (hereafter, the LBOX region). In this simulation, the influence of all external-forcing errors in the two chosen fields is removed by having the influx of energy and water vapor outside the chosen region updated with analyzed winds and soil moisture. This is equivalent to running a regional model with the best available input of humidity and winds from 4DDA analysis. Therefore, C5 must be compared to C4 and C1. Case C5 has large similarities with case C4 and in some respects it is even a better simulation than all the others. Figure 8a shows that the precipitation field gives a better simulation of the magnitude of the observed drought extending from Canada to the north of the Great Lakes through Wyoming, although the orientation of the drought west of 90°W is somewhat poorer. The magnitudes are somewhat smaller

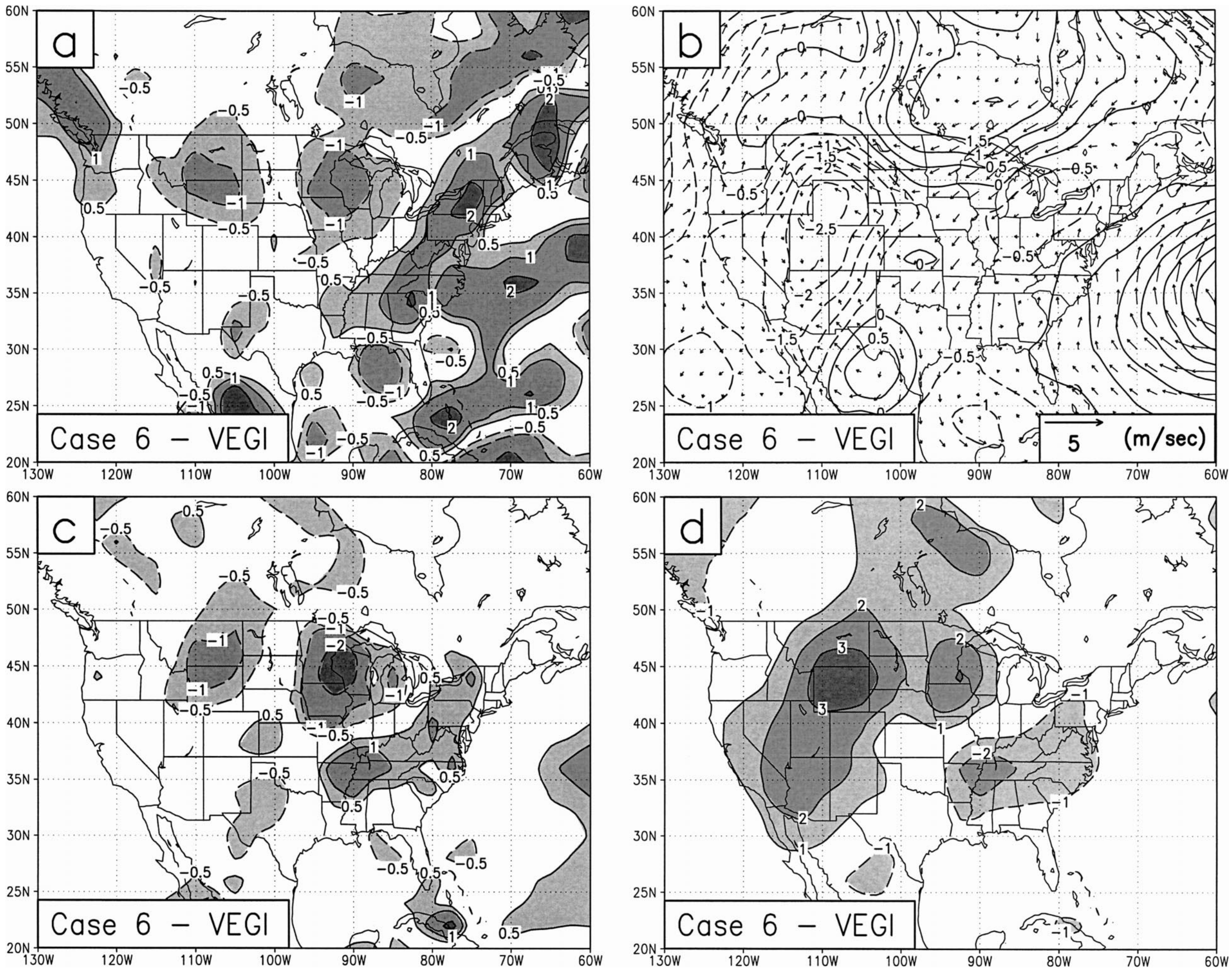

FIG. 9. Same as in Fig. 4 only for case C6 VEGI.

than that of C4, which is an improvement. The primary midwestern drought region has synoptic-scale character, but it is equally well/poorly simulated in both C4 and C5, that is, the deficiencies and strengths of both are similar. The only difference is that magnitudes of case C5 are smaller and are in better agreement with data. The changes in other areas are unremarkable. In C2 and C4, the wind fields were prescribed everywhere, but in C5 it is only prescribed outside the box; consequently, its SLPs (Fig. 8b) were degraded as compared to C4 or C2. This implies that model-introduced errors inside the dynamically free box make SLPs drift away from observations (as expected). The case with prescribed winds and soil moisture (C4) had very little interensemble variability, whereas case C5 has much more (although not nearly as much as C1). This drift is related to the model's freedom to evolve its own circulation and hydrologic processes in the region. Figure 8c shows evapotranspiration anomalies. GSWP evapotranspiration anomalies (Fig. 4c) are much smaller than that of cases C4 and C5. In the higher latitudes, where there is enough soil moisture, 1988 minus 1987 JJA evapotranspiration anomalies are not so large. However, in the midwestern drought regions the anomalies follow the analyzed precipitation-governed initial soil moisture for case C4 and the simulated precipitation for case C5. The surface temperature anomalies (Fig. 8d) are dependent upon winds, cloudiness (affecting solar radiation reaching the surface as well as net outgoing longwave radiation), and evapotranspiration. Since winds are prescribed, the only remaining degrees of freedoms are cloudiness and soil moisture, which produce the observed effects.

### *f. Cases C6 and C7: Same as case C5 with observed vegetation inside LBOX*

In view of a number of sensitivity studies highlighting the importance of biosphere–atmosphere interaction (e.g., Sud et al. 1995), we examine how useful is the GEOS model's sensitivity in simulating the drought circulation. Figure 9a shows that with actual vegetation data, the drought in the Midwest shrank somewhat more

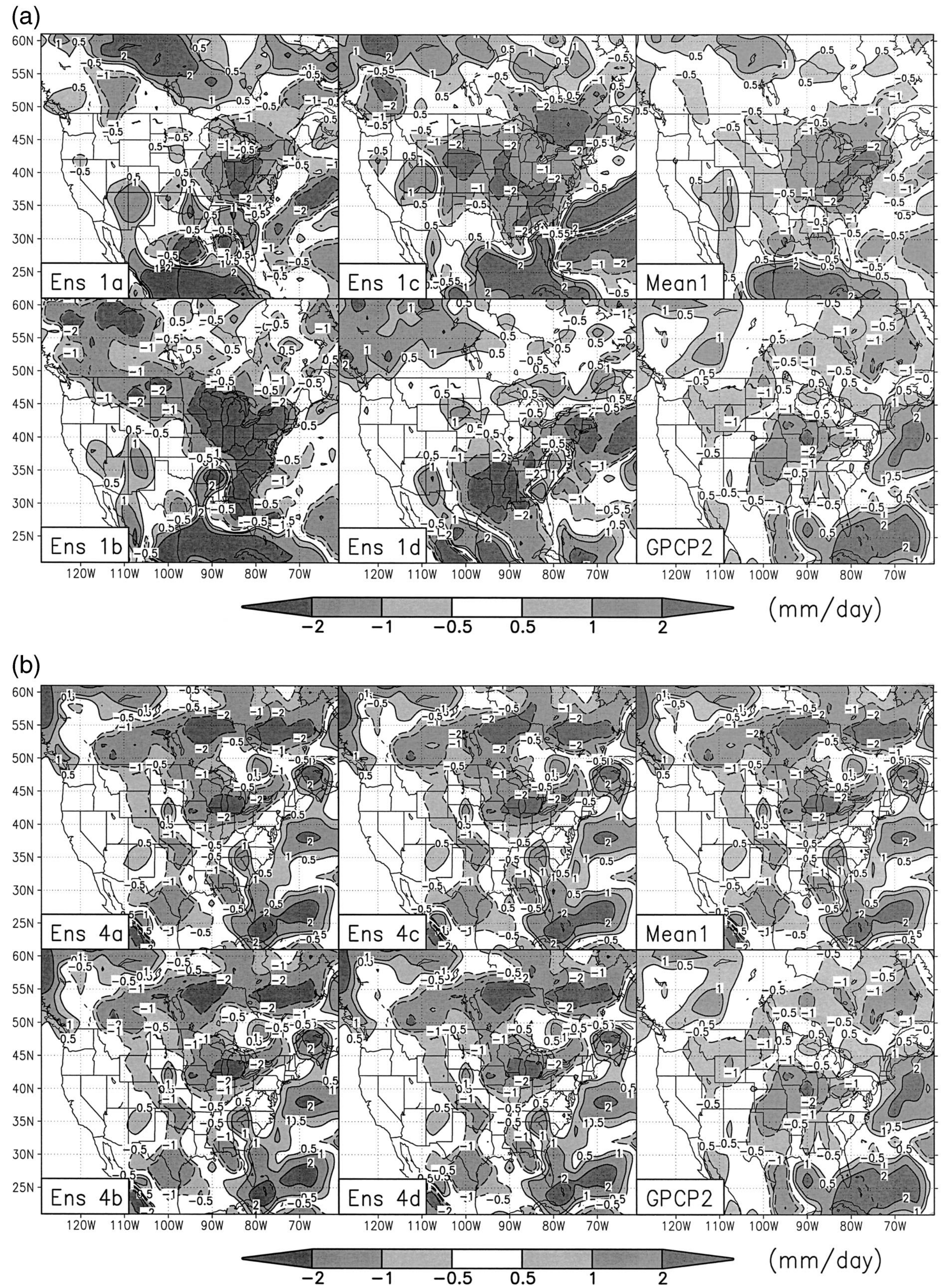


FIG. 10. (a) The 1988 − 1987 JJA precipitation (mm day$^{-1}$) from (top right) case C1 CTRL, (bottom right) GPCP version 2, and (left and center) four individual members from case C1 CTRL ensemble. Negative differences are surrounded by a dash. (b) Same as in (a) only for case C4 BOTH. (c) Same as in (a) only for case C5 LBOX.

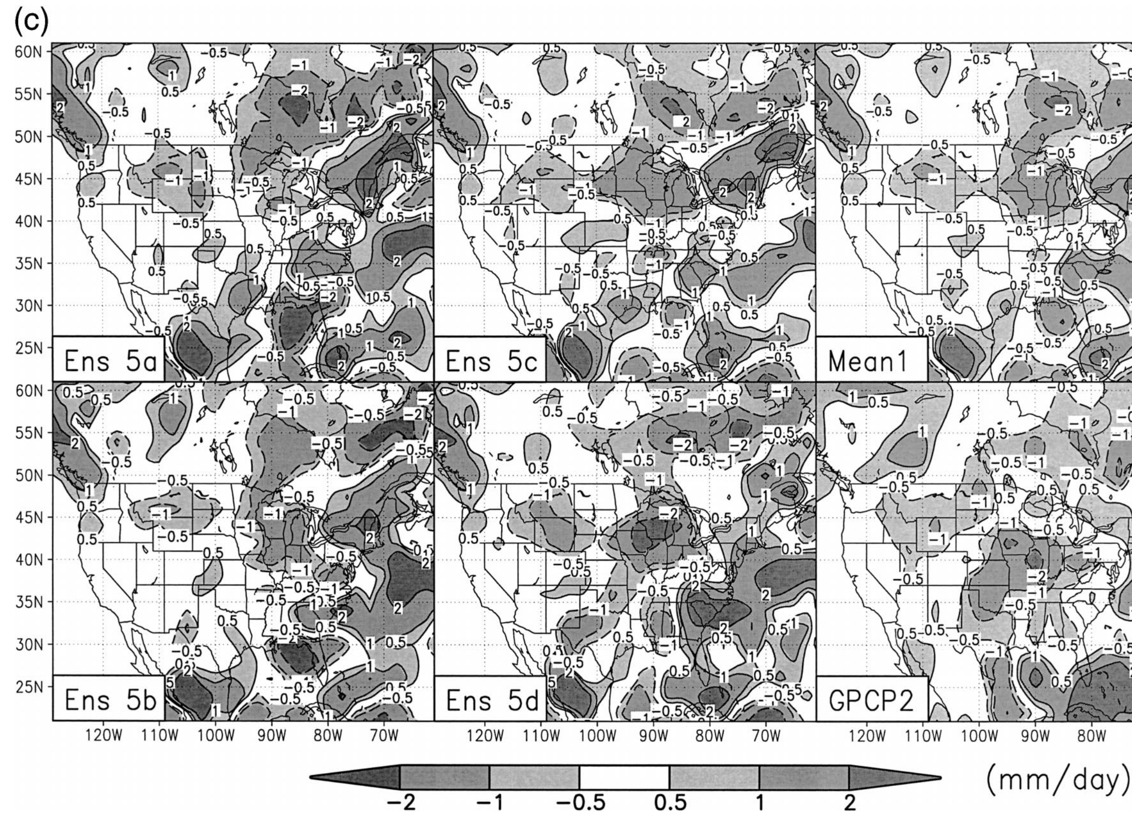


FIG. 10. (*Continued*)

than that of case C5 as compared to the analysis of observations. In addition, the east coast of North America was wetter than that of C4, which itself was wetter than the rainfall in the GPCP data (Fig. 4a). In this respect, the observed vegetation did not help. In the SLP fields (Fig. 9b), the differences between C5 and C6 are unremarkable. The evapotranspiration anomalies in Fig. 9c mimic rainfall anomalies, suggesting that if one simulates large errors in the rainfall, the evapotranspiration (through soil-moisture feedback) will change correspondingly regardless of vegetation parameters. In this simulation many other parameters that are associated with the modified vegetation could not be realistically altered. However, since the parameters modified are considered to be the dominant modulators of evapotranspiration, this should not affect the findings. It would be expected that the drought vegetation parameters of C6, which are less than in C5, will cause less evapotranspiration; however, even this does not happen because the biospheric feedback interactions are so complex that changing the parameters did not affect the time-mean rainfall realistically to make much difference to the simulation. On the other hand, the rainier east coast produced higher evapotranspiration and cooler surface temperatures (Fig. 9d). Case C7 (with opposite year's vegetation data) was very similar to C6 as far as JJA 1988 minus 1987 rainfall, SLP, and winds from surface to 800 hPa, evapotranspiration and surface temperatures (not shown). Thus, there were no discernible differences in the simulation as a consequence of the observed (C6) versus incorrect (C7) vegetation data. The comparison between C5 and C6 showed a slight influence of vegetation on the simulation, while C7 showed virtually no effect, mainly as a consequence of the ISLSCP vegetation data for 1987 and 1988 being closer in agreement to each other than either was to the vegetation data used in the GEOS GCM's climatology for cases C1–C5. Dirmeyer (2000) with the Center for Ocean–Land–Atmosphere Studies (COLA) GCM, which has essentially the same SSiB, has shown that correct soil moisture helped in 1987 and 1988 soil moisture–switched simulations (indeed, it does so in our model as well, not shown), but the more realistic vegetation effect is really small as compared to the circulation and soil moisture effects.

### *g. Analysis of individual cases in the ensemble*

The 1988 minus 1987 JJA precipitation for the four individual ensemble members for case C1 are shown in Fig. 10a. The right two panels of this figure show the mean of the four members (top) and the GPCP analysis (bottom). For simulations C1-a and C1-d, the drought is simulated mainly over the Midwest and eastern United

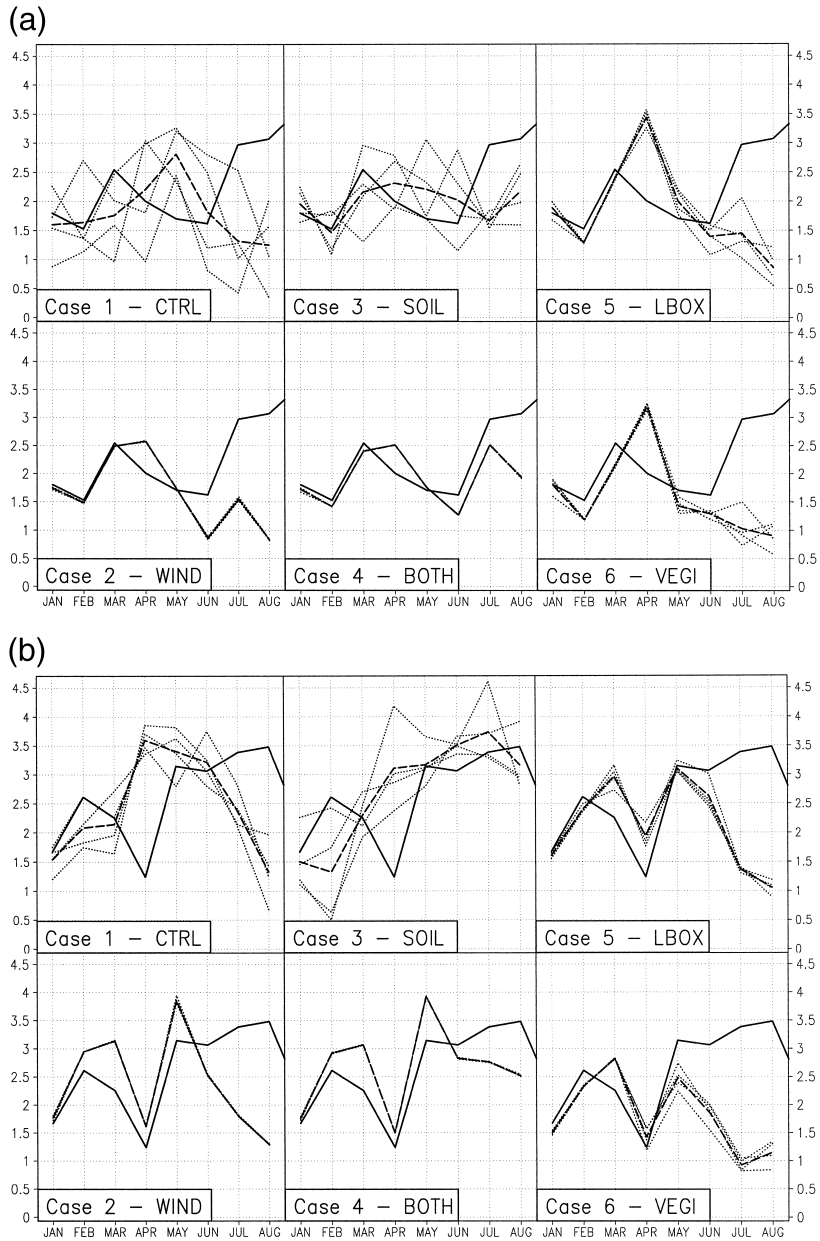


FIG. 11. (a) The 1988 monthly and area-averaged precipitation (mm day$^{-1}$) from cases C1–C6 and GPCP version 2 (solid line) for the central plains area of 30°–50°N and 100°–85°W. The ensemble average is shown with the long dash, and the individual ensemble members are shown with the short dash. (b) Same as in (a) only for 1987.

States. However, the other two ensemble members simulate a widespread drought also over the Great Plains across the northern Rockies. This figure demonstrates both the ability of the GCM to predict a drought 6–8 months in advance (in response to realistic prescription of SST), as well as the uncertainty in predicting its location accurately.

For case C4, Fig. 10b shows how strongly the precipitation anomaly is constrained by just replacing the simulated wind and soil moisture fields with the analyzed wind and soil moisture fields. Very minor differences can be noted, but the general pattern of a drought in the upper Midwest to Great Plains and around the Great Lakes into eastern Canada is virtually identical among all four ensemble members as well as the GPCP panel. For case C5 (Fig. 10c), with winds and soil moisture replaced outside the LBOX region only, greater interensemble differences are found, but not nearly as large as in case C1.

The individual ensemble members were also analyzed with a cyclone tracking routine of Terry and Atlas (1996) for JJA for cases C1, C4, and the reanalysis (not shown). Results from the reanalysis showed no significant difference in the location or frequency of cyclones between 1987 and 1988 during this period. Furthermore, almost no cyclone activity was identified in the northern Great Plains during both years. Similar results were found for case C4, with all four ensemble members having very similar cyclone tracks, as a result of the replaced winds. In the control case C1, several cyclones among all ensemble members were noted in this region during both years, as well as considerable scatter between individual members. This not only points to the expected inability of the model to simulate cyclone tracks in an integration started months in advance, but it also highlights model biases in simulating these tracks.

### *h. Behavior of regional averages*

Monthly averaged precipitation plots for cases C1–C6 for the Great Plains region of 30°–50°N and 85°–100°W for 1988 are shown in Fig. 11a. The figures are shown to detail the month-by-month evolution of the simulations through the spring and summer. The solid line represents the GPCP data and the thick dashed line represents the ensemble average for that case. The four thin dashed lines are the precipitation for each individual ensemble member. For case C1, the average shows that on the whole, the GCM failed to both simulate the strong spring and early-summer drying, as well as the late-summer return of the precipitation in this subregion. The GCM was too wet in the late spring largely due to a poorly simulated circulation, while it was too dry in the late summer from a positive feedback of progressively lower soil moisture in this region. Large differences between ensemble members are found. For cases C2 and C4, strong interensemble member similarity is noted; however, in C2 the late-summer precipitation is again poorly reproduced. The addition of soil moisture data in C4 somewhat helps to simulate better late-summer precipitation. The soil moisture also had a positive effect on simulated precipitation in C3. Case C5 also shows the problem with late-summer drying affecting the precipitation, with the individual ensemble members being much more similar to each other. Adding the correct vegetation data in case C6 somewhat reduced the anomalous high early-spring precipitation and the low late-summer precipitation also shown in C5. The errors in simulated precipitation for all cases tend to be larger than the variability between the ensemble members. Figure 11b shows the same data for 1987 with no spring and early-summer precipitation drought found in the observations. Results from the GCM are generally similar to 1988 with the addition of soil moisture data helping the simulation of late-summer precipitation, and the box region tightly constraining the simulations, but not simulating the late-summer precipitation adequately.

Daily averaged soil moisture data for the Illinois region bounded by 38°–41°N and 88°–92°W for 1988 are shown in Fig. 12a. Here the solid line represents the soil wetness from the offline HY-SSiB analysis forced with the ISLSCP Initiative I data, which had been previously shown to well reproduce observations of soil moisture in this region (Sud and Mocko 1999). In the control case C1, the model tended to keep the soil wetter than observed in midsummer. Again, a large scatter is evident amongst ensemble members in the control case C1. When the winds are replaced in case C2, the stronger than observed summer drying of the soil is seen. The simulated soil moisture is very close to the observed in cases C3 and C4 as a result of replacing soil moisture data daily, but the effect of free-running winds is noted with the numerous soil moisture spikes in C3 before the daily replacement. Cases C5 and C6 agree with previous results, with a moderate amount of scatter and error. In Fig. 12b, the soil-moisture feedback error is further highlighted. In case C2, the late-summer soil moisture is much drier than observed, as it is in C1, C5, and C6.

The spatial correlation of the monthly averaged precipitation between the various cases (C1–C7) for the GEOS model and the GPCP precipitation data for the LBOX region is shown in Table 1. For the control case C1, the correlation is poor for each individual summer month as well as the JJA average. Updating the wind data in C2 greatly improves the precipitation correlation, although the correlation degrades as the summer progresses. In case C3, the soil moisture analyzed data makes a small improvement over the control, while in Case C4, with both winds and soil moisture, the individual month correlation is the highest for all cases, especially into August. Again, the LBOX case of C5 shows a moderate improvement over the control in this area through the use of the remote forcings, as well as cases C6 and C7 showing little change from C5.

## 5. Discussion and conclusions

As discussed in the introduction, the drought of 1988 has not been simulated realistically by any general circulation model. One of the primary reasons for this is the circulation and rainfall biases in the GCM overwhelm the observed anomalies. Indeed, the assumption that biases will cancel out in anomaly minus control simulations did not help much beyond what one sees in the control case. The drought's physical description, together with the available data analysis to date, shows that its causes could be the SST anomalies (both tropical and extratropical) of 1988, a ridge that developed as a result of the past evolution of weather that persisted through the summer, as well as the soil-moisture–vegetation–rainfall feedback. In Sittel's analysis (1994), 40 yr of rainfall and SST data analysis has identified the very same regions of North America for the occurrence of droughts in response to SST anomalies. Therefore, a GCM can potentially simulate the drought in response

(a)

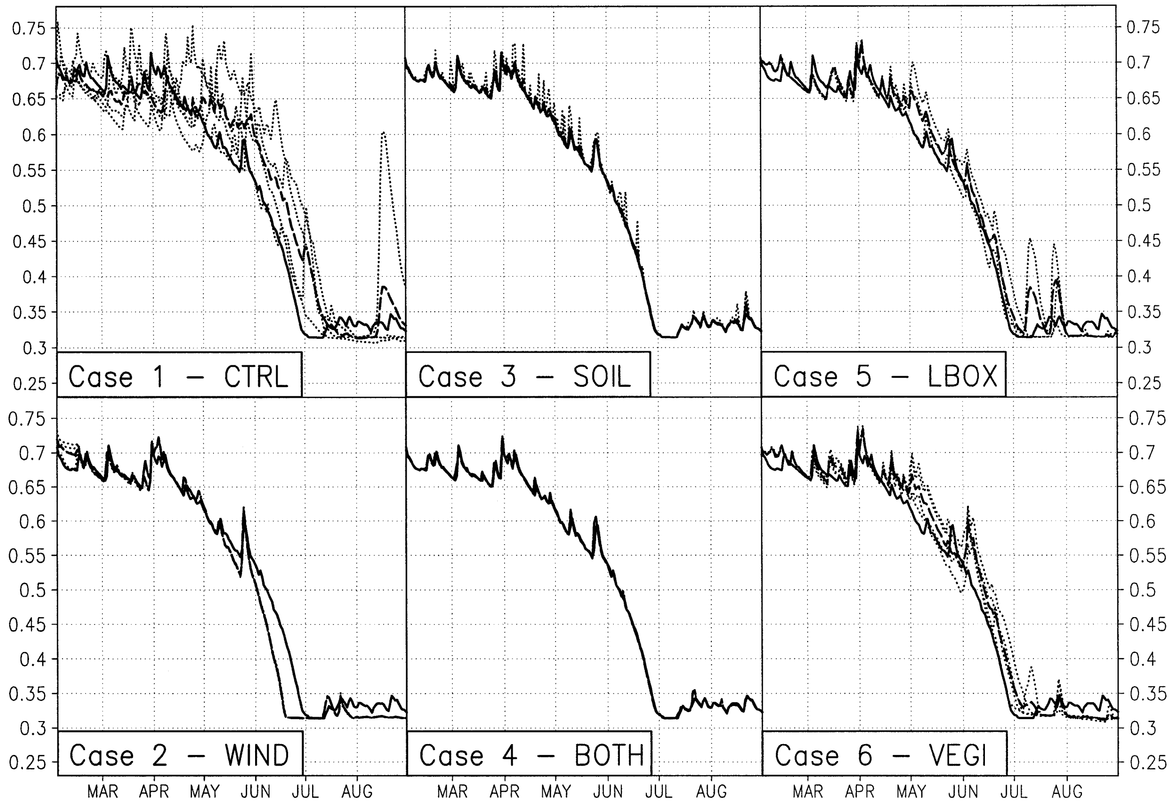
0.75
0.7
0.65
0.6
0.55
0.5
0.45
0.4
0.35
0.3
0.25
Case 1 – CTRL
Case 3 – SOIL
Case 5 – LBOX
Case 2 – WIND
Case 4 – BOTH
Case 6 – VEGI
MAR
APR
MAY
JUN
JUL
AUG

(b)

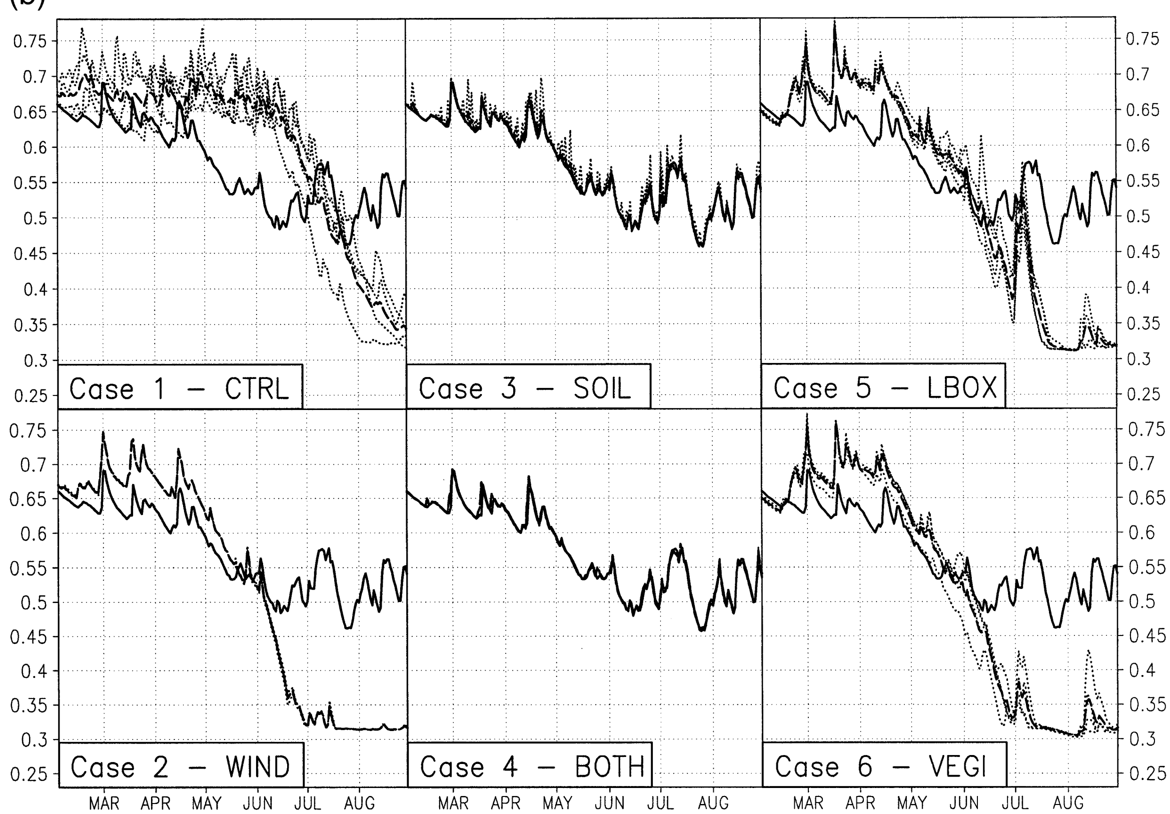
0.75
0.7
0.65
0.6
0.55
0.5
0.45
0.4
0.35
0.3
0.25
Case 1 – CTRL
Case 3 – SOIL
Case 5 – LBOX
Case 2 – WIND
Case 4 – BOTH
Case 6 – VEGI
MAR
APR
MAY
JUN
JUL
AUG

to realistic SSTs, analyzed soil moisture, and partially prescribed circulation.

In our study, the influence of initial conditions is not examined. The feedbacks enter into the system through different modes of winds and soil moisture data ingestions. When only the SST anomalies were prescribed, the GCM did produce some of the circulation features of a drought over North America, but these features could be identified only on the planetary scales. The 1988 minus 1987 precipitation fields show that the GCM was successful in reducing precipitation for the JJA period, but the accompanying circulation anomalies were so poor that one is likely to infer that the GCM simulated the dry conditions for the wrong reason. To isolate the causes for the above behavior, winds and soil moisture were prescribed from analyses of observations as continuous updates to the simulation. Other fields such as temperature, humidity, and/or surface pressure could not be used without invoking full data assimilation.

The results show that much of the simulation biases emanate from wind biases that are carried into the North American region from surroundings areas. When using analyzed winds, only the rotational part of the circulation remains in the system, while the divergent part is strongly modulated by the model's physics, particularly the radiation and latent heating processes. With winds prescribed at 6-h intervals, the interensemble variability of the simulations virtually vanishes. As expected, assimilated winds produce a much better simulation of both the precipitation and low-level circulation at the model's resolution. Inclusion of soil moisture also helps to ameliorate the excessive feedback between soil moisture and precipitation that produced large precipitation anomalies in the control case. The remaining differences between the observed and simulated precipitation and surface temperatures are presumably caused by errors in the model's physics, which includes the cloud–radiation interaction, the precipitation physics and microphysics itself, and the land–atmosphere interaction. The simulations showed the structure of surface temperature and precipitation errors in response to winds alone, soil moisture alone, and both. For the case of prescribed winds, the surface temperature anomalies have one persistent pattern, whereas for the soil moisture it is another. In the combined case, the two patterns merge and help to yield somewhat more realistic evapotranspiration and precipitation patterns. Observing System Simulation Experiments (OSSEs) can better address the question about the influence of model physics on the drought simulation (see Atlas et al. 2003).

The cyclone track analysis did not show a useful difference between 1987 and 1988 for JJA, in either the GCM or the reanalysis. The cyclones tend to be weaker and less frequent in the summer months, and both the observations and model show a strong precipitation deficit in 1988 despite little change in cyclones. Thus, the cyclones of this period produced only a small amount of the precipitation in the Great Plains, which is in agreement with Fritsch et al. (1986) who showed that mesoscale convective systems (MCSs) account for 30%–70% of the summertime precipitation. In the current configuration, the GCM parameterizes moist convection and is unable to resolve MCSs; therefore, we were unable to examine the strength and frequency of MCSs in this region for both years.

Case C5 with the LBOX region without updating soil moisture and winds inside the region, while outside the region winds and soil moisture were updated as in case C4, showed the following. Even though the simulation is substantially different, the forecast quality of case C5 is similar to that of case C4. It shows that many of the local simulation errors originate outside the LBOX region. This can be an expected, because if weather and climate have global connectivity, then any chaotic component of weather can naturally propagate into a region such as LBOX from outside; however, such a large magnitude of this connectivity, even on a seasonal scale, is a surprising new result. Even though we cannot comment on the robustness of this finding for other models, one naturally expects it would not be too different for other state-of-the-art climate models. The new result also reaffirms how and why regional models in a research mode run with prescribed lateral transports from observational data are able to do a more realistic job of simulating a specific phenomenon, while a global model is less constrained and continues to have problems. However, in the long run, only a free-running GCM will enable scientists to predict climate. In that spirit, this research is not an end in itself, but helps to provide guidance on the important issues to face in a GCM exercise. One naturally wonders—since weather is not deterministically predictable beyond 5–10 days, will its time-mean (climate) also contain a significant component of unpredictability over the chosen 3 months (JJA). The question boils down to finding out if the model's biases, which also contribute to the lack of predictability, are so large as to limit the value of its predictions. On the other hand, the model is not sensitive to drought or nondrought vegetation parameters. Clearly, vegetation and soil moisture go together, but if the role of soil moisture dominates the outcome, then its biases would mask any plausible advantage of using the observed vegetation. Dirmeyer (2000) provided the ''correct'' versus the ''opposite'' soil moisture and found a

←

FIG. 12. (a) The 1988 daily and area-averaged root zone soil wetness from cases C1–C6 and GSWP offline (solid line) for the Illinois area of 38°–41°N, and 92°–88°W. The ensemble average is shown with the long dash, and the individual ensemble members are shown with the short dash. (b) Same as in (a) only for 1987.

discernible improvement in response to correct soil moisture. Our results (that are also based on SSiB for the land model) also show that the soil moisture governs the outcome of land–atmosphere feedback interaction much more than the vegetation parameters.

The model's biases in the prescribed soil moisture simulations as well as in the prescribed wind simulations are quite persistent. From this study, we conclude that model biases significantly influence the prediction errors. These biases, through wind errors, change the transports of heat and moisture into the LBOX region. When winds are prescribed from analysis of observations outside the chosen LBOX region, the model produces a much better JJA drought as compared to the control, and it remains almost as good as the one in which winds and soil moisture were prescribed everywhere. This shows that biases in circulation and advective transports propagate and strongly contribute to the simulation biases. Single column model (SCM) simulation research (Ghan et al. 2000; Xie et al. 2002) shows significant model-physics-dependent biases among the participating models even over a single-grid cell; therefore, the authors conclude that the only meaningful way to improve these GCMs is to first reduce their biases at the grid-cell level. This would require improvements in cloud physics, cloud–radiation interactions, boundary layer processes, as well as the rest of the atmospheric column physics. Without such a concerted effort in model improvement, simulating climatic events will continue to be a hit-or-miss prediction. Consequently, GCM-simulated global change inferences will continue to be unreliable. Furthermore, even when the model realistically forecasts a climate event, scientists will ponder about the right/wrong reason for the success, and that in turn will haunt modelers attempting to simulate global-change scenarios.

In the series of simulation attempts reported above, the model is able to predict the very large scale circulation changes as seen in the 200-hPa streamfunction differences of 1988 minus 1987 for JJA somewhat reasonably over North America, which leads to a (somewhat misplaced) midwestern drought in 1988 minus 1987 rainfall. However, the rest of the circulation is not well reproduced. Presumably, soil moisture, which has a much longer timescale than precipitation, (but can be affected by a single weather event, whose course is largely unpredictable), is modulating the ensuing circulation. Even when the soil moisture is prescribed from GSWP analysis of hydrometeorological data from analysis of observations for 1987 through 1988, the evapotranspiration errors remain large. This implies that the net radiation at the surface and vertical temperature and humidity structures that are governed by thermodynamics and vertical-column adjustment physics of the model are contributing to the biases. In fact, if cloud distribution or cloud–radiative feedback are erroneous, net radiation at the surface would be affected and that will influence the evapotranspiration and Bowen ratio. It appears there are significant modeling errors associated with not being able to simulate the drought well, even when winds and soil moistures are prescribed everywhere.

Finally, in our modeling studies to discern the influence of different feedback interactions on simulating the drought of 1988 over North America, the results had a sobering influence on our enthusiasm to use GCMs to simulate climate variations successfully on the North American continental scale. As discussed in the introduction, the failure is not unique to the GEOS GCM. Moreover, since none of the ensemble members' simulated climate change was distinctly similar to the observed, the argument that the observed climate anomaly "scenario" is only a single member of the plausible ensembles of nature does not seem to explain the failure. On the other hand, interensemble biases remain similar; this points to a potentially large contribution by model biases. Therefore, the only way to achieve better success is to reduce, even if unable to eliminate, model biases element-by-element on well-designed parameterization improvement test beds such as Atmospheric Radiation Measurement Program Cloud and Radiation Test Bed (ARM-CART) and GSWP/ISLSCP (already underway). Through such parameterization improvements of the past as well as use of higher resolution, we now have succeeded to produce a much more realistic simulation of seasonal climate. We have also done a fairly decent job of simulating the Indian drought of 1987 with the GEOS GCM (Sud and Walker 1999b), but with respect to the North American drought of 1988, the model's failures have remained remarkably distinct. In this study, we better identified its source causes; however, a better solution must still wait for now.

*Acknowledgments.* We thank both anonymous reviewers for highly constructive suggestions for improvement of the paper. Under their Global Modeling and Analysis Program, NASA HQ provided funding support for this research. This enabled participation of our coauthor, D. M. Mocko, at a substantial level. J. Terry of the NASA Goddard DAO provided assistance with storm track analysis.

## REFERENCES

Atlas, R., N. Wolfson, and J. Terry, 1993: The effect of SST and soil moisture anomalies on GLA model simulations of the 1988 U.S. summer drought. *J. Climate,* **6,** 2034–2048.

——, and Coauthors, 2001: The effects of marine winds from scatterometer data on weather analysis and forecasting. *Bull. Amer. Meteor. Soc.,* **82,** 1965–1990.

——, G. D. Emmitt, J. Terry, E. Brin, J. Ardizzone, J.-C. Jusem, and D. Bungato, 2003: Recent observing system simulation experiments at the NASA DAO. Preprints, *Seventh Symp. on IOS: The Water Cycle, 83d Annual Meeting of the AMS,* Long Beach, CA, Amer. Meteor. Soc., CD-ROM, 2.2.

Castro, C. L., T. B. McKee, and R. A. Pielke, 2001: The relationship of the North American monsoon to tropical and North Pacific sea surface temperatures as revealed by observational analyses. *J. Climate,* **14,** 4449–4473.

Chou, M.-D., and M. J. Suarez, 1994: An efficient thermal infrared radiation parameterization for use in general circulation models.

Goddard Space Flight Center NASA Tech. Memo. 104606, Vol. 3, 102 pp.
——, M. J. Suarez, C.-H. Ho, M.-H. Yan, and K.-T. Lee, 1998: Parameterizations for cloud overlapping and shortwave single scattering properties for use in general circulation and cloud ensemble models. *J. Climate,* **11,** 202–214.
——, K.-T. Lee, S.-C. Tsay, and Q. Fu, 1999: Parameterization of cloud longwave scattering for use in atmospheric models. *J. Climate,* **12,** 159–169.
Conaty, A. L., J. C. Jusem, L. Takacs, D. Keyser, and R. Atlas, 2001: The structure and evolution of extratropical cyclones, fronts, jet streams, and the tropopause in the GEOS general circulation model. *Bull. Amer. Meteor. Soc.,* **82,** 1853–1867.
Dirmeyer, P. A., 1999: Assessing GCM sensitivity to soil wetness using GSWP data. *J. Meteor. Soc. Japan,* **77,** 367–385.
——, 2000: Using a global soil wetness dataset to improve seasonal climate simulation. *J. Climate,* **13,** 2900–2922.
——, A. J. Dolman, and N. Sato, 1999: The pilot phase of the Global Soil Wetness Project. *Bull. Amer. Meteor. Soc.,* **80,** 851–878.
Fennessy, M. J., and J. Shukla, 1999: Impact of initial soil wetness on seasonal atmospheric prediction. *J. Climate,* **12,** 3167–3180.
——, and ——, 2000: Seasonal prediction over North America with a regional model nested in a global model. *J. Climate,* **13,** 2605–2627.
——, J. Kinter, and A. Vernekar, 1990: *Proceedings of the Workshop on the 1988 United States Drought, 30 April–2 May, 1990.* Department of Meteorology, University of Maryland, 201 pp.
Fox-Rabinovitz, M. S., L. L. Takacs, R. C. Govindaraju, and M. J. Saurez, 2001: A variable resolution stretched-grid general circulation model: Regional climate simulation. *Mon. Wea. Rev.,* **129,** 453–469.
Fritsch, J. M., R. J. Kane, and C. R. Chelius, 1986: The contribution of mesoscale convective weather systems to the warm-season precipitation in the United States. *J. Climate Appl. Meteor.,* **25,** 1333–1345.
Ghan, S., and Coauthors, 2000: A comparison of single column model simulations of summertime midlatitude continental convection. *J. Geophys. Res.,* **105** (D2), 2091–2124.
Giorgi, F., L. O. Mearns, C. Shields, and L. Mayer, 1996: A regional model study of the importance of local versus remote controls of the 1988 drought and the 1993 flood over the central United States. *J. Climate,* **9,** 1150–1162.
Helfand, M. H., and J. C. Lebraga, 1988: Design of a non-singular level 2.5 second-order closure model for prediction of atmospheric turbulence. *J. Atmos. Sci.,* **45,** 113–132.
Hong, S.-Y., and H.-L. Pan, 2000: Impact of soil moisture anomalies on seasonal, summertime circulation over North America in a Regional Climate Model. *J. Geophys. Res.,* **105** (D24), 29 625–29 634.
Huffman, G. J., and Coauthors, 1997: The Global Precipitation Climatology Project (GPCP) Combined Precipitation Dataset. *Bull. Amer. Meteor. Soc.,* **78,** 5–20.
Jenkins, G. S., and E. J. Barron, 2000: Regional climate simulations over the continental United States during the summer of 1988 driven by a GCM and the ECMWF analyses. *Global Planet. Change,* **25,** 19–38.
Karl, T. R., P. Y. Groisman, R. W. Knight, and R. R. Heim, 1993: Recent variations of snow cover and snowfall in North America and their relation to precipitation and temperature variations. *J. Climate,* **6,** 1327–1344.
Lau, K.-M., K.-M. Kim, and S. S. P. Shen, 2002: Potential predictability of seasonal precipitation over the United States from canonical ensemble correlation predictions. *Geophys. Res. Lett.,* **29,** 1097, doi:10.1029/2001GL014263.
Meeson, B. W., F. E. Corprew, J. M. P. McManus, D. M. Myers, J. W. Closs, K.-J. Sun, D. J. Sunday, and P. J. Sellers, 1995: *ISLSCP Initiative I—Global Data Sets for Land–Atmosphere Models, 1987–1988.* Vols. 1–5, NASA CD-ROM.
Mo, K. C., J. R. Zimmerman, E. Kalnay, and M. Kanamitsu, 1991: A GCM study of the 1988 United States drought. *Mon. Wea. Rev.,* **119,** 1512–1532.
Mocko, D. M., and Y. C. Sud, 2001: Refinements to SSiB with an emphasis on snowphysics: Evaluation and validation using GSWP and Valdai data. *Earth Interact.,* **5,** 1–31.
——, G. K. Walker, and Y. C. Sud, 1999: New snow-physics to complement SSiB. Part II: Effects on soil moisture initialization and simulated surface fluxes, precipitation, and hydrology of GEOS 2 GCM. *J. Meteor. Soc. Japan,* **77,** 349–366.
Namias, J., 1991: Spring and summer 1988 drought over the contiguous United States—Causes and prediction. *J. Climate,* **4,** 54–65.
Pal, J. S., and E. A. B. Eltahir, 2001: Pathways relating soil moisture conditions to future summer rainfall with a model of the land–atmosphere system. *J. Climate,* **14,** 1227–1242.
Schubert, S. D., R. B. Rood, and J. Pfaendtner, 1993: An assimilated dataset for Earth science applications. *Bull. Amer. Meteor. Soc.,* **74,** 2331–2342.
Shen, S. S. P., K.-M. Lau, Kim, G. Li, and A. Basist, 2002: Formulation of the canonical ensemble correlation prediction for seasonal precipitation. *Chin. J. Atmos. Sci.,* **26,** 114–140.
Sittel, M., 1994: Differences in the means of ENSO extremes for temperature and precipitation in the United States. COAPS Tech. Rep. 94-2, 50 pp.
Sud, Y. C., and A. Molod, 1988: A GCM simulation study of the influence of Saharan evapotranspiration and surface-albedo anomalies on July circulation and rainfall. *Mon. Wea. Rev.,* **116,** 2388–2400.
——, and D. M. Mocko, 1999: New snow-physics to complement SSiB. Part I: Design and evaluation with ISLSCP Initiative 1 datasets. *J. Meteor. Soc. Japan,* **77,** 335–348.
——, and G. K. Walker, 1999a: Microphysics of Clouds with the Relaxed Arakawa–Schubert Scheme (McRAS). Part I: Design and evaluation with GATE Phase III data. *J. Atmos. Sci.,* **56,** 3196–3220.
——, and ——, 1999b: Microphysics of Clouds with the Relaxed Arakawa–Schubert Scheme (McRAS). Part II: Implementation and performance in GEOS II GCM. *J. Atmos. Sci.,* **56,** 3121–3240.
——, W. C. Chao, and G. K. Walker, 1993: Dependence of rainfall on vegetation: Theoretical considerations, simulation experiments, observations, and inferences from simulated atmospheric soundings. *J. Arid Environ.,* **25,** 5–18.
——, K.-M. Lau, G. K. Walker, and J.-H. Kim, 1995: Understanding biosphere–precipitation relationships: Theory, model simulations, and logical inferences. *MAUSAM,* **46,** 1–14.
——, G. K. Walker, V. Mehta, and K.-M. Lau, 2002: Relative importance of the annual cycles of sea surface temperature and solar irradiance for tropical circulation and precipitation: A climate model simulation study. *Earth Interact.,* **6,** 1–32.
Takacs, L. L., A. Molod, and T. Weng, 1994: Documentation of the Goddard Earth Observing System (GEOS) General Circulation Model—Version 1. Goddard Space Flight Center NASA Tech. Memo. 104606, Vol. 1, Greenbelt, MD, 100 pp.
Terry, J., and R. Atlas, 1996: Objective cyclone tracking and its applications to *ERS-1* scatterometer forecast impact studies. Preprints, *15th Conf. on Weather Analysis and Forecasting,* Norfolk, VA, Amer. Meteor. Soc., 146–149.
Trenberth, K. E., and G. W. Branstator, 1992: Issues in establishing causes of the 1988 drought over North America. *J. Climate,* **5,** 159–172.
——, and C. J. Guillemot, 1996: Physical processes involved in the 1988 drought and 1993 floods in North America. *J. Climate,* **9,** 1288–1298.
——, G. W. Branstator, and P. A. Arkin, 1988: Origins of the 1988 North American drought. *Science,* **242,** 1640–1645.
Xie, S.-C., and Coauthors, 2002: Intercomparison and evaluation of cumulus parameterizations under summertime midlatitude continental conditions. *Quart. J. Roy. Meteor. Soc.,* **128,** 1095–1136.
Xue, Y., P. J. Sellers, J. L. Kinter III, and J. Shukla, 1991: A simplified biosphere model for global climate studies. *J. Climate,* **4,** 345–364.
Zhou, J., Y. C. Sud, and K.-M. Lau, 1996: Impact of orographically induced gravity–wave drag in the GLA GCM. *Quart. J. Roy. Meteor. Soc.,* **122,** 903–927.